Aalborg Universitet

AALBORG UNIVERSITY

Lifetime Estimation of Electrolytic Capacitors in Fuel Cell Power Converter at Various Confidence Levels

Zhou, Dao; Wang, Huai; Blaabjerg, Frede

Link to publication from Aalborg University

Lifetime Estimation of Electrolytic Capacitors in a Fuel Cell Power Converter at Various Confidence Levels

Dao Zhou, Huai Wang, and Frede Blaabjerg

Department of Energy Technology
Aalborg University
Pontoppidanstraede 101, Aalborg, DK-9220, Denmark
zda@et.aau.dk, hwa@et.aau.dk, fbl@et.aau.dk

Abstract - **DC capacitors in power electronic converters are a major constraint on improvement of the power density and the reliability. In this paper, according to the degradation data of tested capacitors, the lifetime model of the component is analyzed at various confidence levels. Then, the mission profile based lifetime expectancy of the individual capacitor and the capacitor bank is estimated in a fuel cell backup power converter operating in both standby mode and operation mode. The lifetime prediction of the capacitor banks at different confidence levels is also obtained.**

I. INTRODUCTION

Fuel cell system is emerging as an important candidate to substitute conventional technologies used in backup power system (e.g. generator set, or battery system), thanks to its high specific energy, high reliability, and no pollution [1], [2]. Due to the variable dc voltage with respect to the load current, the energy system based on fuel cell source need to be regulated in order to achieve high-quality supply of power [3]. In general, the capacitors play a vital role in the operation of power electronic converters, which are one of the most susceptible elements to failure among other components [4].

In respect to the design of capacitors in power converter, it embraces many considerations (like voltage rating, ripple current rating, power loss and stability). In fact, large capacitance values have been observed to make the dc voltage more robust. In [5], the value of the dc-link capacitance for motor drive is selected based on the theoretical maximum power that could be supplied to the capacitor over a single switching period. On the other hand, the value of the dc-link capacitance is chosen based on the rise time and maximum allowed overshoot of the dc-link voltage control [6]. To our knowledge, there are few studies concerning the effects on capacitors from the loading conditions, while the mission profile based research is of intense interest for power electronic converter [7].

Since reliability statistics are using a sample space to predict the trends of a whole population, it is quite natural to

expect a certain degree of uncertainty, and this is the origin of the confidence level, which defines the probability that the value of a parameter falls within a specified range [8]. Among previous studies [7], [9]-[11], the lifetime estimation of the reliability-critical components in power electronic converters is a specific value, which is usually at 50% confidence level. This paper introduces an approach to configure the lifetime model at different confidence bounds from the original degradation data.

This paper addresses the lifetime estimation of the capacitor bank used in a fuel cell system at various confidence levels. Section II describes the mission profile of the backup power supply system. The lifetime model of the radial electrolytic capacitor is derived from the testing data in respect to the temperature stress in section III. Afterwards, the component-level and system-level lifetime expectancy of the capacitors are calculated in section IV. Finally, the concluding remarks are drawn in the last section.

II. MISSION PROFILE OF BACKUP POWER CONVERTER

In order to cope with the wide-range output voltage of a fuel cell stack, a 1 kW galvanic isolated power converter with two independent transformers is applied as shown in Fig. 1, to supply a regulated output voltage for telecom applications [12]. The aluminum electrolytic capacitors are used in the front-end and the rear-end of the power converter with the purposes of the smooth input voltage and the reasonable ripple of the

Table I
POWER CONVERTER SPECIFICATION AND PARAMETERS

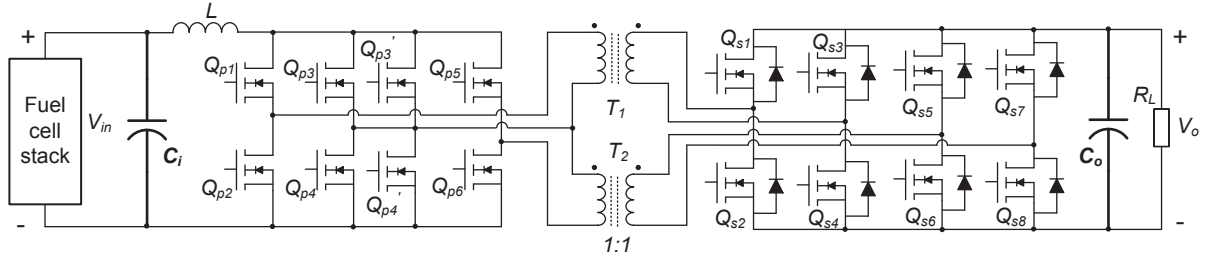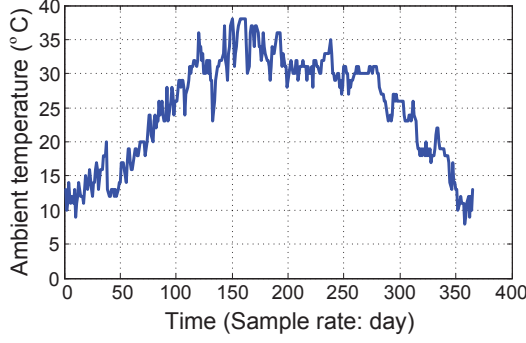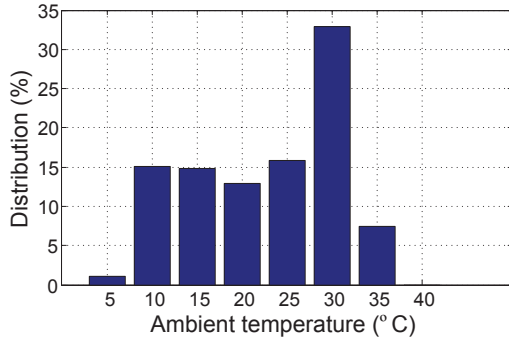|	
Input voltage V_{in}	30 – 65 V
Output voltage V_o	48 V
Maximum output power P_o	1000 W
Primary-side MOSFETs	100 V/74 A, ×8
Secondary-side MOSFETs	100 V/74 A, ×8
Input capacitor C_i	390 μF/100 V, ×6
Output capacitor C_o	680 μF/63 V, ×8
Input inductor L	15 μH
Transformer ratio n	1:1
Switching frequency f_{sw}	50 kHz

Fig. 1. Isolated dc/dc power converter used in the fuel cell telecom backup power.
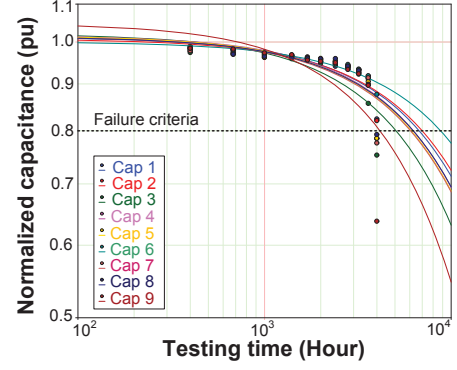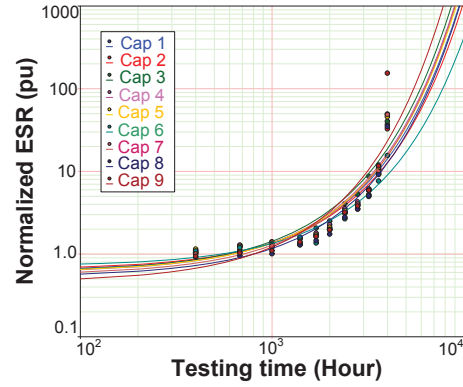

(a)

(b)

Fig. 2. Annual temperature profile in the case of severe application. (a) Temperature profile with one sampling data per day; (b) Temperature distribution.

(a)

(b)

Fig. 3. Capacitor degradation testing results at the rated voltage, rated ripple current and upper operational temperature for 9 capacitors. (a) Normalized capacitance; (b) Normalized ESR.

output voltage – 6 input capacitors (C_i) of the 390 µF/100 V and 8 output capacitors (C_o) of 680 µF/ 63 V. Other key parameters of the power converter are listed in Table I.

In respect to the backup power, two main working modes can be identified. The power converter mainly works in the standby mode when the power grid is in normal operation, while the power converter is activated in the operation mode at the presence of the power outages. Consequently, the stability of the power grid is an essential mission profile, and a daily outage with four-hour duration can be expected for severe users [12]. For the sake of simplicity, a typical telecom loading profile is 10-hour full load and 2-hour quarter load periodically, as stated in [13]. The annual ambient temperature is shown in Fig. 2, and it can be further described by the different temperature ranges.

III.   FAILURE DATA AND LIFETIME MODEL OF TESTED ELECTROLYTIC CAPACITOR

The change in capacitance, Equivalent Series Resistance (ESR), dissipation factor, and leakage current are considered as key indicators during the healthy condition of the electrolytic capacitors [4]. To obtain the time-to-failure distribution of the applied capacitors, a degradation test is performed with a series of 9 capacitors (56 µF/35 V) at the rated voltage, upper operational temperature (105 °C) and rated ripple current, and the normalized capacitance and ESR are regularly measured during the 4,000 testing hours. As shown in Fig. 3, the results are analyzed by using the software tool Weibull++ [14]. It can be observed that the capacitance values drop and the ESR values increase during the testing.
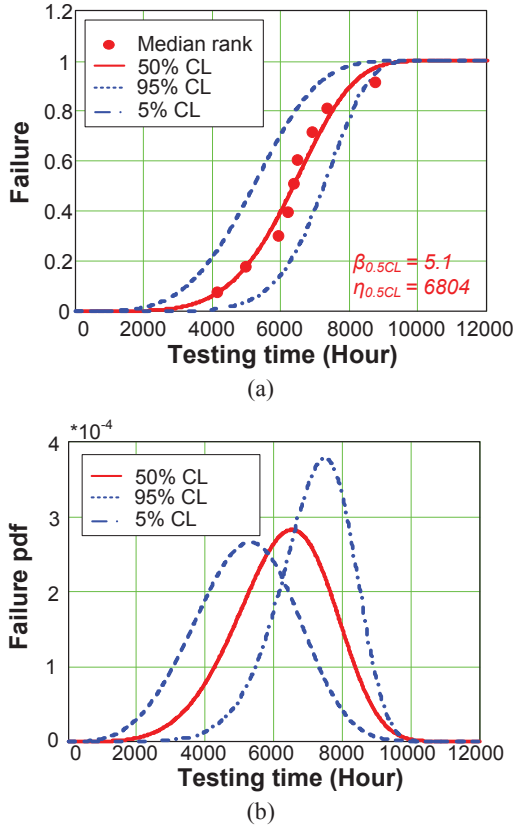
Fig. 4. Time-to-failure of capacitors at different Confidence Levels (CL) by using Weibull distribution in the case of 105 ºC. (a) Failure along with testing time; (b) Probability Density Function (pdf) of failure.

20% of capacitance drop is used as the end-of-life criteria since the reduction speed of the capacitance increase significantly after the capacitance values reach of 80% of their initial values.

The deterministic reliability in a certain type of capacitors is not obtainable due to the testing results in a number of samples from the total population. Confidence levels are introduced to describe the statistical properties of reliability or lifetime information obtained from testing results of a limited number of samples [14].

The Median Rank (MR) for the jth failure in N tested units is the value that the probability the jth failure occurs before its corresponding time is 50%, which equals to 50% confidence level [14]. Assuming that each test is an independent event, which obeys the binomial distribution, its failure rate Z can be obtained by solving the following cumulative binomial distribution,

$$P = \sum_{k=j}^{N} \binom{N}{k} Z^k (1-Z)^{N-k} \qquad (1)$$

where P is the confidence level, N is the sample size, j is the order number, and Z is the ranking value.

As a consequence, if 50% confidence level (P=0.5) is considered, the MR for each failure item can be calculated by solving (1) with the changing failure number. Moreover, if the two-side 90% confidence bounds are required, (1) must be solved twice (P=0.05 and P=0.95) in order to place the bound around 90% of the population.

By using the MR, 9 discrete samples are located in Fig. 4(a). As mentioned in [14], the key parameters of Weibull distribution can be found by using the probability plotting method, the least square method (rank regression), or the maximum likelihood estimation. A shape factor of 5.1 and a scale factor of 6,804 can be read with the help of the rank regression approach. Similarly, the confidence levels of 95% and 5% are taken into account, the fitting Weibull distribution in these cases can be obtained, and they are also shown in Fig. 4(a). Furthermore, the probability density function (pdf) of the failure is calculated in Fig. 4(b). As the B_X lifetime corresponds to the time when $X\%$ of the population fails, it is noted that the B_X lifetime can be different in the case of the various confidence levels.

As discussed in [4], [15], a typical form of lifetime model of electrolytic capacitors is given by,

$$L = L_0 \cdot 2^{\frac{T_0 - T}{n_1}} \left(\frac{V}{V_0}\right)^{-n_2} \qquad (2)$$

where L_0 and L are the lifetime at the reference condition and the used condition, V_o and V are voltage at the reference condition and the used condition, and T_0 and T are the temperature at the reference condition and the used condition, respectively. n_1 is the temperature dependence constant, and n_2 is the voltage stress exponent. According to leading capacitor manufacturers [15], n_2 equals 0 for the small-size radial type capacitors if the applied voltage is below rated voltage, as the temperature-dependent electrolyte loss is the dominant failure mechanism. Meanwhile, n_1 equals 10. According to the above information, the lifetime at different temperature levels below the upper operational temperature can be estimated.

IV. COMPONENT-LEVEL AND SYSTEM-LEVEL LIFETIME ESTIMATION OF CAPACITORS

This section presents an approach to estimate the expected lifetime for the input-side capacitors (C_i) and output-side capacitors (C_o) shown in Fig. 1 in the cases of standby mode and operation mode. Besides, the lifetime estimation of the individual capacitor further contributes to the system-level by using the reliability block diagram, in which the confidence bound is also taken into account as well.

The applied capacitors for input-side and output-side are in the same series as the tested capacitors discussed in Section II, with a rated lifetime of 5,000 hours stated in the datasheet. The reliability information as shown in Fig. 4 is suitable for both the input capacitors and the output capacitors.
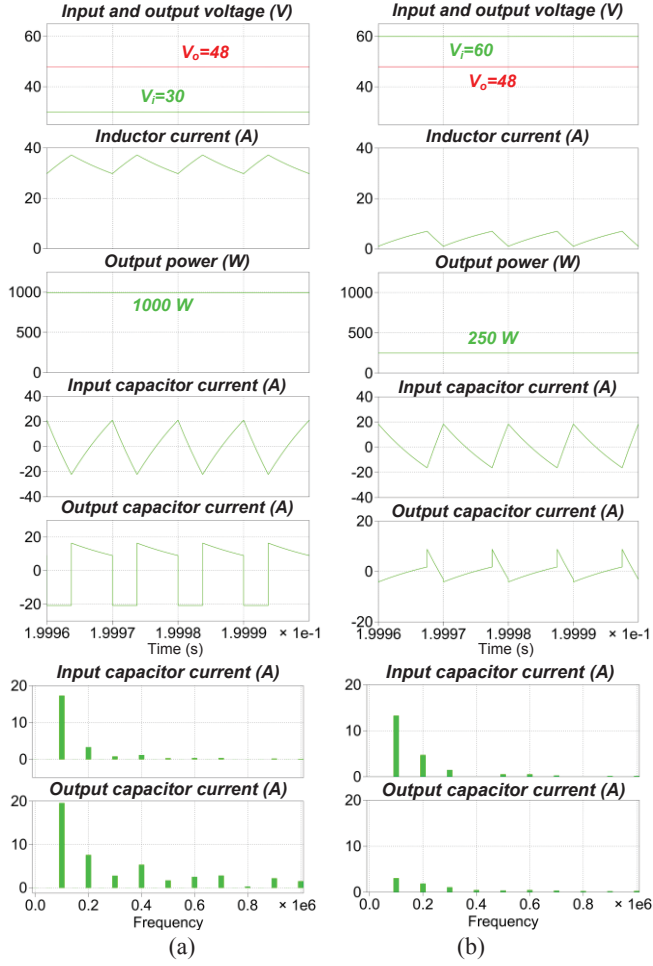
Fig. 5. Voltage and current stresses of input and output capacitor banks at different loading conditions for the circuit in Fig. 1. (a) 1000 W; (b) 250 W.

In the case of the standby mode, the capacitor temperature is assumed to be the ambient temperature. Based on the ambient temperature distribution and the stability of the power grid, the annual damage AD can be calculated by using Miner's rule [16],

$$AD_i = \sum_{i=5}^{35} \frac{Dt_i \cdot Do \cdot 365 \cdot 24}{L_i} \qquad (3)$$

where the subscript i indicates the temperature range from 5 ℃ to 35 ℃ as shown in Fig. 2(b), D_t denotes the percentage of the temperature distribution, D_o denotes the percentage of the power converter working in the standby mode, L denotes the predicted lifetime at the temperature level of i, which can be obtained by using (2).

In the case of the operation mode, the capacitor temperature is jointly determined by the loading condition and the ambient temperature. As previously mentioned, the power converter operates either in the quarter loading or in the full loading in a typical telecom application. The simulated current of the input
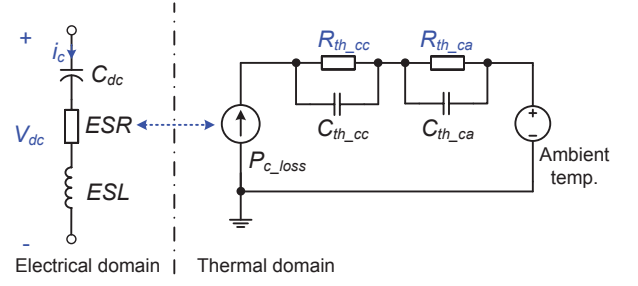

Fig. 6. Relationship between the electrical and thermal models of the electrolytic capacitors.

Table II
PARAMETERS RELATED TO CORE TEMPERATURE ESTIMATION OF THE USED CAPACITORS

	Type	EEUFC1J681
Output capacitor	Dimension (mm)	12.5×35
	ESR (mΩ)	141
	Temperature rise (℃)	27.6
Input capacitor	Type	EEUFC2A391
	Dimension (mm)	16×35.5
	ESR (mΩ)	159
	Temperature rise (℃)	45.0
Thermal resistance from core to case		8.33 ℃/W
Thermal resistance from case to ambient		18.15 ℃/W

and output capacitors are shown in Fig. 5. It is noted that the harmonic spectrum of the capacitor current is mainly dominated by double switching frequency components.

As shown in Fig. 6, the power loss of the capacitor is caused by the ripple current across the ESR. Besides, the temperature of the capacitor can be estimated based on its thermal impedance and cooling solutions. As listed in Table II, with the ESR and the thermal resistance of the used capacitors, the temperature rise of the capacitor can be obtained. It is worth noting that since the outage duration lasts four hours, the power converter has to work in the full load according to the loading profile of the telecom power. The temperature rise of the input capacitor and the output capacitor are 45.0 ℃ and 27.6 ℃, respectively. As a result, the annual damage in the operation mode can be calculated according to (3).

Based on the failure data, the damage of the output-side capacitor is shown in Fig. 7, in which the standby mode and the operation mode are compared. As the loading condition leads to the capacitor temperature rise of 27.6 ℃, if B_1 lifetime model is considered, the higher core temperature in the operation mode causes a higher annual damage of 1.41E-2 compared to the standby mode of 1.05E-2, which indicates a lifetime of 41 years. Similarly, the same approach can be extended to the input-side capacitor, and the B_1 lifetime can be calculated as 17 years.

In order to predict the reliability metrics from each component to the whole capacitor bank used in the power converter, a reliability block diagram [8] is adopted and its structure is shown in Fig. 8. As aforementioned, the input
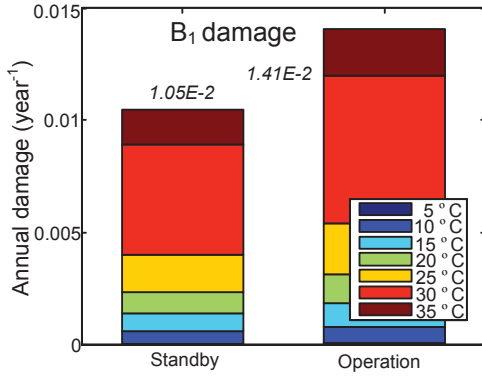
Fig. 7. B_1 annual damage of the output-side capacitor in the cases of the standby mode and operation mode.
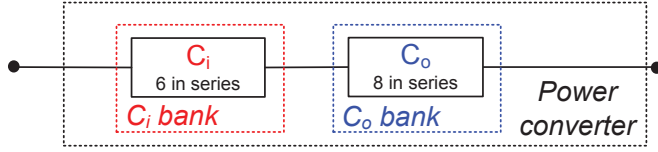

Fig. 8. Reliability block diagram from each capacitor to the capacitor bank in the power converter shown in Fig. 1.

capacitor bank has 6 capacitors in parallel and the output capacitor bank contains 8 capacitors.

Based on the B_1 lifetime of the input-side and output-side capacitor marked in Fig. 9(a), it can be seen that the shape parameter of 5.1 equals to the tested capacitor lifetime shown in Fig. 4 due to the same failure mechanism with different scale parameter. Since the failure of each capacitor causes the faulty operation of the power converter, the reliability function is connected in series and the reliability of the capacitor bank is the sum of the individual capacitor. As the backup power application is with very stringent reliability requirement, only B_1 lifetime is considered for the capacitors. It can be observed although the B_1 lifetime of the individual input and output capacitor are 17 and 41 years, the B_1 lifetime of their capacitor bank is remarkably reduced to 12 and 26 years, respectively.

As the reliability function of capacitors used in the fuel cell power converter is the sum of input capacitor bank and the output capacitor bank, the system-level capacitor lifetime can be calculated in Fig. 9(b). Meanwhile, the zoom-in system-level lifetime distribution of the capacitor is shown in Fig. 9(c). It is noted that the B_1 lifetime of the capacitor system is 12 years by using the Median ranking. However, if the two-side 90% confidence bound is considered, the lifetime is distributed between 8 and 21 years.
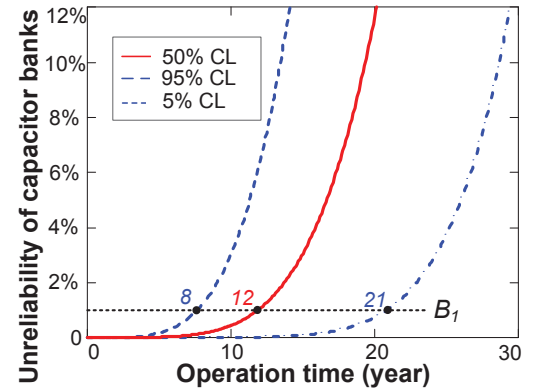
V. CONCLUSION

This paper starts with a mission profile description of the fuel cell power converter used in backup power application in terms of ambient temperature, the grid stability and the loading condition. Based on the test data of the electrolytic capacitors at the upper operation temperature, the reliability
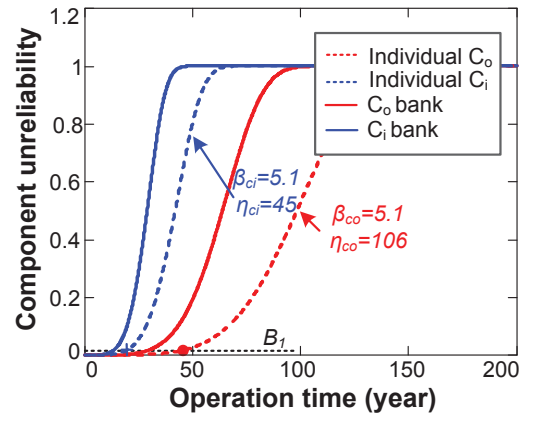
(a)
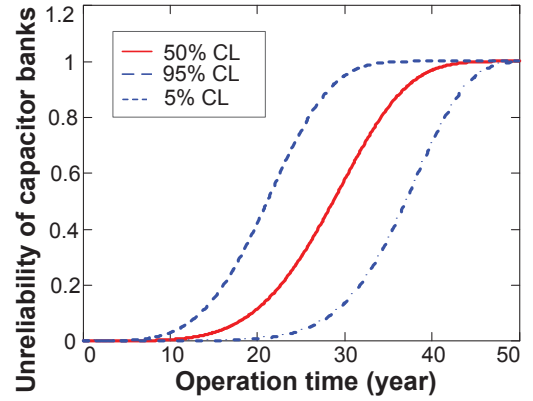
(b)

(c)

Fig. 9. Lifetime estimation of capacitors in the fuel cell power converter. (a) Component-level reliability; (b) System-level reliability considering the confidence bound; (c) Zoom-in of system-level reliability. Note: CL denotes the confidence level

model can be derived, and it can be further extended to any temperature level by using a typical lifetime model from the leading capacitor manufacturers. With the help of B_1 lifetime model, the relevant annual damage can be calculated in the case of the standby mode and the operation mode. Afterwards, the component-level reliability of the input capacitor and output capacitor can be estimated. By using the reliability block diagram, the system-level lifetime of the capacitor bank

can be predicted with various confidence levels. It is evident that the B_1 lifetime of the whole capacitor bank is 12 years with the confidence level of 50%. With a 90% confidence level, the B_1 lifetime is in a range between 8 years and 21 years, i.e. statistically, it has a 95% probability that the capacitor banks have a minimum B_1 lifetime of 8 years.

References

[1] K. Rajashekara, "Hybrid fuel-cell strategies for clean power generation," *IEEE Trans. on Industry Applications*, vol. 41, no. 3, pp. 682-689, May 2005.

[2] M. Jang, and V. G. Agelidis, "A minimum power-processing-stage fuel-cell energy system based on a boost-inverter with a bidirectional backup battery storage," *IEEE Trans. on Power Electronics*, vol. 26, no. 5, pp. 1568-1577, May 2011.

[3] M. J. Vasallo, J. M. Andujar, C. Garcia, and J. J. Brey, "A methodology for sizing backup fuel-cell/battery hybrid power systems," *IEEE Trans. on Industrial Electronics*, vol. 57, no. 6, pp. 1964-1975, Jun. 2010.

[4] H. Wang, and F. Blaabjerg, "Reliability of capacitors for DC-link applications in power electronic converters—an overview," *IEEE Trans. on Industry Applications*, vol. 50, no. 5, pp. 3569-3578, Sep. 2014.

[5] L. Malesani, L. Rossetto, P. Tenti, and P. Tomasin, "AC/DC/AC PWM converter with reduced energy storage in the DC link," *IEEE Trans. on Industry Applications*, vol. 31, no. 2, pp. 287-292, Mar. 1995.

[6] T. Messo, J. Jokipii, J. Puukko, and T. Suntio, "Determining the value of DC-link capacitance to ensure stable operation of a three-phase photovoltaic inverter," *IEEE Trans. on Power Electronics*, vol. 29, no. 2, pp. 665-673, Feb. 2014.

[7] K. Ma, M. Liserre, F. Blaabjerg, and T. Kerekes, "Thermal loading and lifetime estimation for power device considering mission profiles in wind power converter," *IEEE Trans. on Power Electronics*, vol. 30, no. 2, pp. 590-602, Feb. 2015.

[8] P. D. T. O'Connor, and A. Kleyner, *Practical Reliability Engineering (fifth edition)*. New York, USA: Wiley, 2012.

[9] Y. Yang, H. Wang, F. Blaabjerg, and K. Ma, "Mission profile based multi-disciplinary analysis of power modules in single-phase transformerless photovoltaic inverters," *in Proc. of EPE 2013*, pp.1-10, 2013.

[10] D. Zhou, F. Blaabjerg, M. Lau, and M. Tonnes, "Optimized reactive power flow of DFIG power converters for better reliability performance considering grid codes," *IEEE Trans. on Industrial Electronics*, vol. 62, no. 3, pp. 1552-1562, Mar. 2015.

[11] H. S. Chung, H. Wang, F. Blaabjerg, and M. Pecht, *Reliability of power electronic converter systems*. Institution of Engineering and Technology, 2015.

[12] L. P. Petersen, L. C. Jensen, and M. N. Larsen, "High efficiency isolated DC/DC converter inherently optimized for fuel cell applications," *in Proc. of EPE 2013*, pp.1-10, 2013.

[13] M. J. Vasallo, J. M. Andujar, C. Garcia, and J. J. Brey, "A methodology for sizing backup fuel-cell/battery hybrid power systems," *IEEE Trans. on Industrial Electronics*, vol. 57, no. 6, pp. 1964-1975, Jun. 2010.

[14] Reliasoft Corporation, "*Life data analysis reference*," [Online]. Available: www.reliasoft.com, 2016.

[15] A. Albertsen, "*Electrolytic capacitor lifetime estimation*," [Online]. Available: www.jianghai-america.com, 2016.

[16] H. C. Yildirim, G. Marquis, and Z. Barsoum, " Fatigue assessment of high frequency mechanical impact (HFMI)-improved fillet welds by local approaches," *International Journal of Fatigue*, vol. 52, pp. 57–67, 2013.